

# Spatial uniformity comparison of two nonimaging concentrators

Joseph P. Rice

Yuqin Zong

Daniel J. Dummer

National Institute of Standards and  
Technology

Optical Technology Division  
Gaithersburg, Maryland 20899

E-mail: rice@garnet.nist.gov

**Abstract.** The spatial uniformity of two nonimaging concentrators is measured, each with a silicon photodetector positioned immediately behind the concentrator. The comparison is made between a compound parabolic concentrator (CPC) and a  $\theta_i/\theta_o$  concentrator. The latter consists of a parabolic section followed by a cone section to restrict the divergence angle of the exit beam. The spatial uniformity of the  $\theta_i/\theta_o$  concentrator measured with an  $f/4$  beam diverging from a circular aperture is 1.2% across the central 4 mm of the entrance aperture of the concentrator, and demonstrates the use of this type of concentrator for effectively maintaining high throughput when using small-area (<2-mm-diam) detectors in applications requiring small fields of view. The uniformity of the gold-coated  $\theta_i/\theta_o$  concentrator measured with a nearly collimated HeNe laser beam is not nearly as good, due in part to the imperfect reflectance of gold. The uniformity of the CPC in the  $f/4$  beam is not nearly as good as that of the  $\theta_i/\theta_o$  concentrator in the  $f/4$  beam. © 1997 Society of Photo-Optical Instrumentation Engineers. [S0091-3286(97)00211-0]

Subject terms: infrared radiometric sensor calibration; concentrator; nonimaging; optics; radiometer; radiometry.

Paper RSC-02 received May 15, 1997; revised manuscript received July 7, 1997; accepted for publication July 11, 1997.

## 1 Introduction

Nonimaging concentrators, traditionally used in solar energy collection applications,<sup>1</sup> have properties that also make them useful in radiometric instrumentation applications. One example is for matching detectors to integrating spheres.<sup>2</sup> Another example, which motivated the experiments reported here, is as a self-baffling optic for concentrating light onto a small detector in narrow-field-of-view radiometers.<sup>3</sup> In this application, it was desired to collect and detect all the light in an  $f/4$  beam having a diameter of about 5 mm. However, detector technology limited the largest available detector diameter to about 2 mm. Thus, a nonimaging light concentrator was used instead of a traditional imaging mirror for transforming the large-area, small-solid-angle beam onto the small-area, large-solid-angle beam required for optimum matching to the detector. An advantage of the concentrator over a traditional mirror is that it is self-baffling; that is, since the detector is mounted in close proximity to the exit aperture of the concentrator, light can get to the detector only by traversing the concentrator.

In radiometric applications where a radiometer is used to measure the radiance from a nonuniform source, small displacements of the radiometer relative to the source can lead to systematic errors in the measurement if the radiometer response is not spatially uniform. Thus it is important that the optics used in front of the detector have a design that maintains the spatial uniformity of the radiometer response and minimizes such practical parameters such as size and weight. As part of the design process for such a radiometer, we measured the spatial uniformity of two nonimaging con-

centrators having different designs but approximately the same exit diameters. The choice of similar exit diameter was made since the goal is to match to a detector placed at the exit aperture.

## 2 Concentrator Description

Figure 1 shows two types of concentrators: the traditional compound parabolic concentrator (CPC) design, also known as a Winston cone, and another design, the  $\theta_i/\theta_o$  concentrator.<sup>1</sup> In each case, a detector is placed in close proximity to the exit aperture of the concentrator. This configuration is commercially available with, for example, a liquid-helium-cooled silicon bolometer as the detector. The spatial uniformity of the response to an incident beam, measured across the entrance aperture of these concentrator/detector combinations, is of interest in evaluating the utility of such concentrators in radiometric applications.

The CPC is generated in three dimensions by rotating the parabola  $P'Q'$  (or  $PQ$ ) about the axis of revolution (Fig. 1). Note that the CPC is not simply a paraboloid, since the axis of revolution is at an angle  $\theta_i$  to the axis of the parabola. Also, since the focus of the parabola  $P'Q'$  is the point  $Q$ , meridional light rays that enter the CPC through the entrance aperture  $P'P$  at angle  $\theta_i$  to the axis of the revolution exit the CPC at grazing incidence to the exit aperture  $QQ'$ . Meridional rays entering the CPC with smaller angles of incidence  $\theta_{\text{entrance}}$  exit the CPC within the aperture  $QQ'$ , but the exit angle  $\theta_{\text{exit}}$  varies from 0 to 90 deg from the axis of revolution, depending on  $\theta_{\text{entrance}}$  and the point of incidence at the entrance aperture.<sup>1</sup> Thus, a

**Compound Parabolic Concentrator (CPC):**

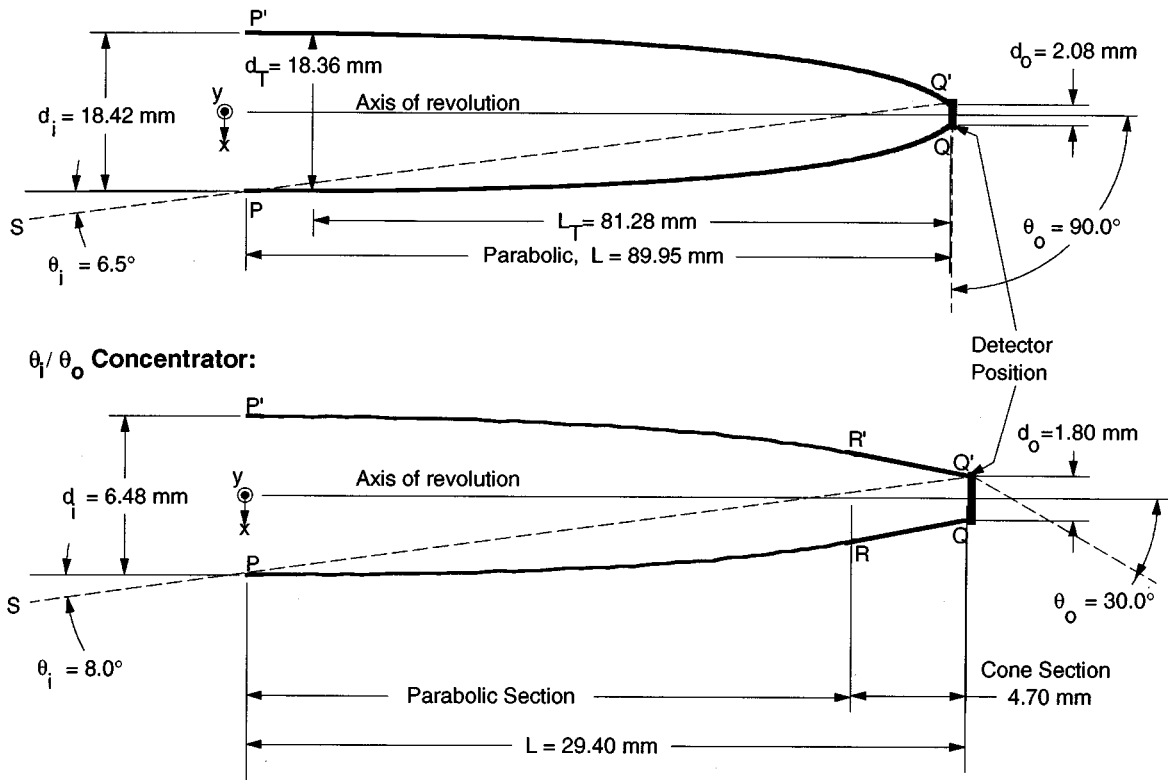


**Fig. 1** Design of the CPC and the  $\theta_i/\theta_o$  concentrator. For the CPC, the parabola  $P'Q'$  has its focus at  $Q$  and its axis parallel to  $SQ'$ . Similarly, for the  $\theta_i/\theta_o$  concentrator, parabola  $P'R'$  has its focus at  $Q$  and its axis parallel to  $SQ'$ , but  $R'Q'$  is a straight line. Each concentrator is generated in three dimensions by rotating  $P'Q'$  about the axis of revolution. Note that the concentrators are drawn to different scales to emphasize the differences near the detector end.

detector must be placed very close to the exit aperture if it is to intersect most of the exiting rays, and incidence angles on the detector range from 0 to 90 deg with respect to the detector normal.

The  $\theta_i/\theta_o$  concentrator consists of a parabolic section followed by a cone section (Fig. 1). The focus of the parabolic section  $P'R'$  is the point  $Q$  and the parabola axis is parallel to  $SQ'$ . The concentrator is generated in three dimensions by rotating the curve  $P'Q'$  (or  $PQ$ ) about the axis of revolution. The parabolic section  $P'R'$  then generates a CPC-like section and the straight line  $R'Q'$  generates a cone. Rays incident on the entrance aperture of the concentrator at angles less than  $\theta_i$  emerge from the exit aperture at angles less than  $\theta_o$ , where  $\theta_i$  and  $\theta_o$  are measured with respect to the concentrator axis of revolution (Fig. 1).

For the  $\theta_i/\theta_o$  concentrator, the entrance aperture diameter  $d_i$  is related to the exit aperture diameter  $d_o$  by<sup>1</sup>

$$d_i = \frac{\sin \theta_o}{\sin \theta_i} d_o, \tag{1}$$

and the total length  $L$  of the concentrator is given by

$$L = \frac{1}{2} (d_i + d_o) \cot \theta_i. \tag{2}$$

Note that these equations are also valid for the CPC with  $\theta_o = 90$  deg.<sup>1</sup>

The particular CPC that we tested was actually a truncated CPC, which is a CPC where part of the entrance aperture end has been removed, giving it a truncated length  $L_T$  and a truncated entrance aperture diameter  $d_T$ . Considerable reduction in length can be achieved with very little difference in performance.<sup>1</sup> For our CPC,  $\theta_i = 6.5$  deg,  $d_o = 2.08$  mm, full entrance aperture diameter  $d_i = 18.42$  mm, truncated entrance aperture diameter  $d_T = 18.36$  mm, full length  $L = 89.95$  mm, and truncated length  $L_T = 81.28$  mm. The CPC was made from electroformed nickel and was electroplated with a reflective layer of gold.

For the particular  $\theta_i/\theta_o$  concentrator that we tested,  $\theta_i = 8$  deg,  $\theta_o = 30$  deg,  $d_i = 6.48$  mm,  $d_o = 1.80$  mm, and  $L = 29.40$  mm. The  $\theta_i/\theta_o$  concentrator was made by electroforming copper on a polished mandrel, then electroplating the inside with an adhesion layer of nickel, followed by electroplating a reflective layer of gold.

Because Fresnel reflection at the detector varies strongly with detector incidence angle at high angles, rays exiting

the concentrator exit aperture at high angles with respect to the axis of revolution have less chance of being absorbed by the detector than rays exiting the concentrator at low angles. This effect would tend to reduce the spatial uniformity of the concentrator-detector combination, since the exit angle of a given ray from the concentrator depends on its position (and angle) at the concentrator entrance. Note that for the CPC design,  $\theta_o$  is fixed at 90 deg, meaning that the rays exiting the CPC are incident on the detector at angles from 0 (normal) to 90 deg with respect to the axis of revolution, whereas for the  $\theta_i/\theta_o$  concentrator the value for  $\theta_o$  can be chosen by design. This enables improved spatial uniformity of the  $\theta_i/\theta_o$  concentrator over the CPC, since a small value  $\theta_o$  can be chosen so that Fresnel reflection at the detector for rays having incidence angle  $\theta_o$  is not significantly different from rays having normal incidence, thus maximizing the spatial uniformity of the concentrator-detector combination. For instance, in the particular  $\theta_i/\theta_o$  concentrator design reported here,  $\theta_o$  was chosen to be 30 deg, since Fresnel reflectance at the detector in our application varies by only a few percent at most up to this angle.

### 3 Experimental Arrangement

For the uniformity tests, the concentrator was mounted with its exit aperture within 0.25 mm of the front surface of a bare silicon photodetector. The detectors used had diameters several times greater than the concentrator exit aperture diameters. A helium-neon laser was used to align the concentrator axis of revolution with the normal to the detector. To achieve the alignment, the mount was adjusted until the laser beam reflected from the bare silicon detector surface overlapped the beam reflected from a flat mirror placed against the entrance aperture  $P'P$  of the concentrator. The concentrator-detector pair was then mounted on an  $x$ - $y$  translation stage using a mount that enabled angular alignment of the pair with respect to the  $z$  (optical axis of the beam) direction.

Spatial uniformity was measured with respect to two different types of optical beams: an  $f/4$  beam and a laser beam. An  $f/4$  beam was chosen because this is within the desired acceptance angle for both concentrators and is approximately the convergence for the radiometric applications for which these concentrators are intended.

### 4 Uniformity with an $f/4$ Beam

The  $f/4$  beam was produced by focusing light from a tungsten filament strip lamp (operated at 15 A and 5.3 V) onto a pinhole aperture using a spherical mirror. A red filter that passes light having wavelengths greater than about 600 nm was placed in the beam just after the lamp. This was done since our interest is in using these gold-coated concentrators in the IR, where the reflectivity of gold is near unity. White light would give unwanted contributions from wavelengths shorter than about 600 nm, where the reflectivity of gold begins to fall. Thus, the spectrum used for probing spatial uniformity ranged from near 600 nm, defined by the red filter, to near 1100 nm, defined by the long-wavelength cutoff of the silicon detector. Two different pinhole aperture diameters were used: one had a diameter of 1 mm and the other had a diameter of 50  $\mu\text{m}$ . In each case, the pin-

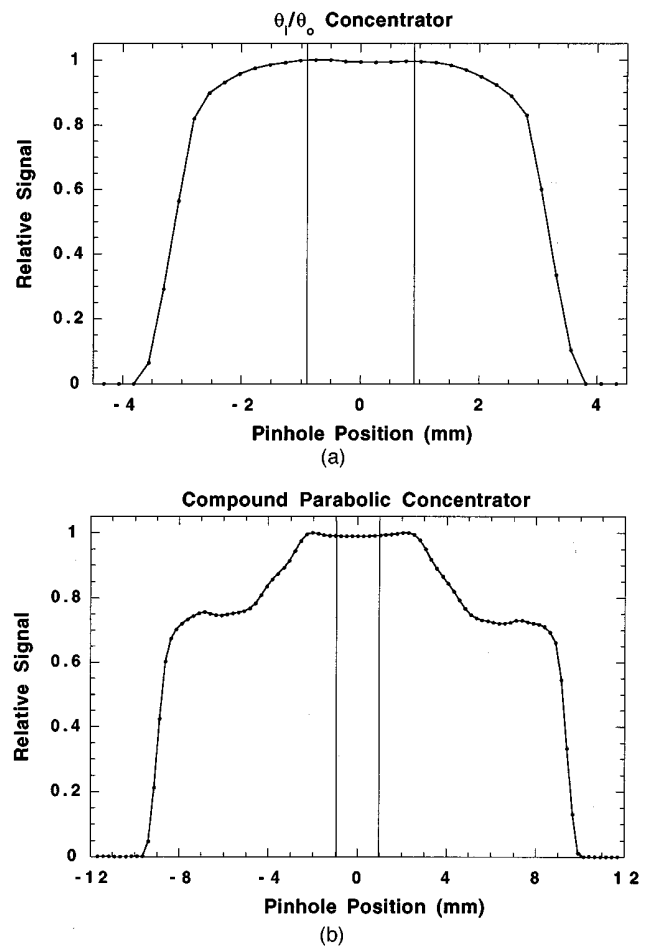


**Fig. 2** Spatial uniformity of the concentrators measured with an  $f/4$  beam and a pinhole aperture diameter of 1 mm. The relative signal values are peak normalized, and the pinhole position is relative to the concentrator axis of revolution. The lines connecting the data points are a guide for the eyes, and the vertical lines indicate the edges of the concentrator exit aperture.

hole aperture was positioned about 1 mm from the entrance aperture of the concentrator. The metal defining the pinhole aperture was blackened to absorb light reflected back from the concentrators. A chopper positioned just after the tungsten lamp chopped the light at 83 Hz. The signal from the silicon detector was preamplified and detected using a lock-in amplifier. The stability of the measured flux was adequate enough that no monitor detector was necessary. A computer controlled the scanning of the  $x$ - $y$  stage and recorded the detected light as measured by the silicon detector. Preliminary scans showed nonsymmetrical patterns indicative of a slight misalignment of the concentrator-detector pair with respect to the beam. After making a fine adjustment, the patterns were symmetrical.

The results of scanning the concentrator-detector combination through the fixed  $f/4$  beam with the 1-mm-diam pinhole aperture for both concentrators are shown in Fig. 2. Shown are  $y$  scans through the centers of the concentrators ( $x=0$ ). Data from  $x$  scans through the center ( $y=0$ ) are not shown but are identical, as expected from symmetry. In Fig. 2(a), data from the  $\theta_i/\theta_o$  concentrator are shown,

whereas in Fig. 2(b) data from the CPC are shown. In both cases, the degree of spatial uniformity is less than that of the silicon detectors alone, and so comparisons can be made between the concentrators. (The spatial uniformity of one of the silicon detectors alone was measured by scanning a laser beam across its active area before mounting the concentrator, and showed a standard deviation of the response of less than 0.3%.) The  $\theta_i/\theta_o$  concentrator exhibits reasonably good spatial uniformity, extending well outside the central area covered by the detector. For the central 4 mm, the spatial uniformity measured as the ratio of the standard deviation of the signal to the mean signal is 1.2%. For the central 5 mm, the uniformity is 3.3%. However, the spatial uniformity for the CPC is not nearly as good. The CPC uniformity suffers from shoulders that develop immediately outside of the central flat region.

Data taken for scanning the  $\theta_i/\theta_o$  concentrator through the  $f/4$  beam with the 50- $\mu\text{m}$ -pinhole aperture were very similar to those shown for the 1-mm-diam-pinhole aperture. For the central 4 mm, the spatial uniformity measured earlier is 1.0%; for the central 5 mm, it is 3.3%. As the beam is scanned away from the central region, the rays that make up the beam must make a greater number of reflections, and the losses increase with the number of reflections. This gradual rolloff is to be expected and is seen for both concentrators. For the CPC, however, a portion of the rays emerge from the concentrator at high angles (out to 90 deg) from the detector normal. Such rays experience near-grazing incidence with the detector, and are thus more likely to be reflected from the detector rather than absorbed. This is not a problem for the  $\theta_i/\theta_o$  concentrator, since the output rays emerge at maximum angle  $\theta_o$  (30 deg for the particular  $\theta_i/\theta_o$  concentrator that we tested) from the detector normal. We believe that this may be one of the reasons for the difference in spatial uniformity seen between the two concentrators.

We have chosen to compare two concentrators having approximately the same size exit apertures, since in the radiometer applications we are considering, the detector is matched to the exit diameter and there is a practical upper limit to detector size; that is, the radiometer designer would choose the detector having the largest available size consistent with a required detector spatial uniformity, then ask what is the most compact concentrator design that would increase the effective area without disturbing spatial uniformity. Our choice necessarily meant that the entrance aperture diameter and length of the CPC that we used were nearly three times greater than those of the  $\theta_i/\theta_o$  concentrator (Fig. 1). Thus, the reader would need to scale our results appropriately to compare concentrators having equal entrance diameters. For example, Fig. 2(b) indicates that the particular CPC we tested could be used to enable a 2-mm-diam detector to act as a reasonably uniform 4-mm-diam detector. However, the CPC would be nearly three times larger than the  $\theta_i/\theta_o$  concentrator that performs the equivalent function. Thus, there can be a practical size and weight advantage to using a  $\theta_i/\theta_o$  concentrator instead of a CPC for radiometer applications.

## 5 Uniformity with a HeNe Laser Beam

To show that the uniformity depends on the beam geometry, a HeNe laser beam (633 nm) was also used to measure

the spatial uniformity of the  $\theta_i/\theta_o$  concentrator. This gives a worst-case estimate, since in our intended applications, the input beam is not collimated so there is significant averaging over a relatively wide range of input angles. The laser beam was chopped at 100 Hz and sent through a beamsplitter, linear polarizer, and lens. The reflected beam from the beamsplitter was directed at a monitor silicon detector. The polarizer provided either horizontal ( $x$  direction) or vertical ( $y$  direction) polarization. The lens shaped the laser beam to a spot size of about 1 mm at the entrance aperture of the concentrator, and the beam was nearly collimated. No pinhole aperture was used. The two signals, one from the silicon detector immediately behind the concentrator and the other from the monitor silicon detector, were each preamplified and detected by individual lock-in amplifiers. A digital voltmeter then monitored the ratio (concentrator detector/monitor detector) of the dc outputs of the lock-in amplifiers as the  $x$ - $y$  translation stage was scanned under computer control. The monitor detector was used in this case to improve temporal stability.

The uniformity results for scanning the  $\theta_i/\theta_o$  concentrator across the HeNe laser beam are shown in Fig. 3. The uniformity differs substantially from that in the  $f/4$  beam case. Immediately away from the central maximum, where most of the beam traverses the concentrator with no reflection from the concentrator surface, the signal drops to a shoulder having a height 60 to 70% of that at the central maximum. The patterns are basically symmetric. The residual asymmetry seen can be attributed to imperfect alignment of the concentrator, detector, and beam. With the polarization in the scan direction [Fig. 3(a),  $x$  scan with  $x$  polarization], the shoulder is 60% of the maximum. For polarization perpendicular to the scan direction [Fig. 3(b),  $x$  scan with  $y$  polarization], the shoulder is 70% of the maximum.

That the level of spatial uniformity depends on the polarization direction is an indicator that the polarization and angle-dependent Fresnel reflectance at the gold concentrator surface are playing a role in causing some of the observed nonuniformity. At high incidence angles, the reflectance of gold is a strong function of polarization direction, as can be determined using the Fresnel reflectance equations to calculate the reflectance from the known optical constants of gold.<sup>4</sup> The reflectance for polarization parallel to the plane of incidence ( $p$ ) is less than that for polarization perpendicular to the plane of incidence ( $s$ ). Thus, the transmittance of the concentrator is expected to be reduced more for  $p$ -polarized light than for  $s$ -polarized light. In Fig. 3, light incident on the concentrator gold surface during the  $x$  scan with  $x$  polarization is primarily  $p$  type, and the shoulder transmittance is 60%, whereas during the  $x$  scan with  $y$  polarization the light is primarily  $s$  type, and the shoulder transmittance is 70%. We say "primarily" here because the concentrator surface is not flat. Thus, as expected, the transmittance is reduced more for the mostly  $p$ -polarized case than for the mostly  $s$ -polarized case.

## 6 Conclusions

The spatial uniformity of the  $\theta_i/\theta_o$  concentrator measured with an  $f/4$  beam is 1.2% across the central 4 mm, and thus

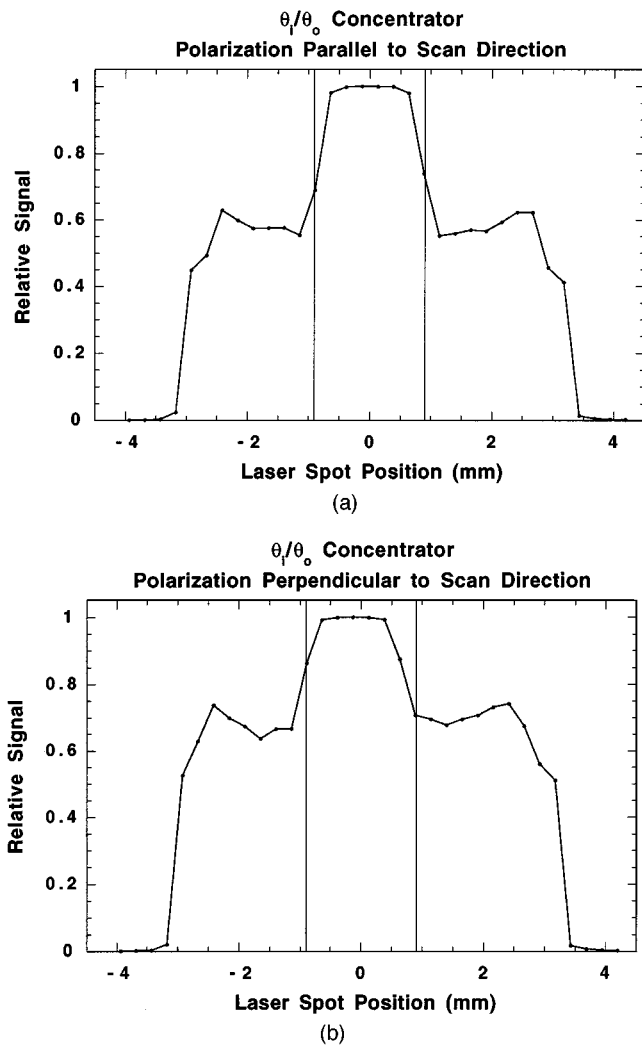


**Fig. 3** Spatial uniformity of the  $\theta_i/\theta_o$  concentrator measured with a HeNe laser beam. The relative signal values are peak normalized, and the laser spot position is relative to the concentrator axis of revolution. The lines connecting the data points are a guide for the eyes, and the vertical lines indicate the edges of the concentrator exit aperture.

enables a 2-mm-diam detector to act as a uniform larger diameter detector with a reduced field of view. However, the spatial uniformity measured with a HeNe laser beam is not as good, falling to 60 to 70% of maximum outside of the central 2 mm. The spatial uniformity of the CPC is not nearly as good as that of the  $\theta_i/\theta_o$  concentrator, in part because of the demands placed on the detector to absorb rays at a high angle of incidence.

### Acknowledgment

We thank L. Hanssen for his advice and encouragement in the use of concentrators in radiometric applications.

### References

1. W. T. Welford and R. Winston, *High Collection Nonimaging Optics*, Academic Press, San Diego (1989).
2. L. Hanssen and K. Snail, "Nonimaging optics and the measurement of diffuse reflectance," *Proc. SPIE* **1528**, 142–150, 1991.
3. J. P. Rice and B. C. Johnson, "A NIST thermal infrared transfer standard radiometer for the EOS program," *Earth Obs.* **8**(3), 31–35 (1996).
4. E. D. Palik, Ed., *Handbook of Optical Constants of Solids*, Academic Press, Orlando, FL (1985).



**Joseph P. Rice** received a BS degree in physics from Iowa State University in 1987 and MS and PhD degrees in solid state physics from the University of Illinois at Urbana-Champaign in 1989 and 1992, respectively. For 2 years he was a postdoctoral research associate with the National Institute of Standards and Technology (NIST) in Boulder, Colorado, where he developed novel IR detectors based on superconductors. Since 1994 he has been a staff member of the Optical Technology Division at NIST in Gaithersburg, Maryland. His research has centered around the development of new types of standard radiometers for a variety of radiometric measurement applications.



**Yuqin Zong** received his BEng in 1984 from Zhejiang University, China, and his MS in optics in 1987 from Institute of Optics and Electronics, Chinese Academy of Sciences. From 1987 to 1994 he was working with space-borne remote sensing radiometers as well as test and calibration equipment at Shanghai Institute of Technical Physics, Chinese Academy of Sciences. He is currently a guest researcher at the National Institute of Standards and Technology. His ongoing projects include visible and IR spectrophotometers, diffraction loss measurements in radiometry, flashing light photometers, and the high accuracy cryogenic radiometer.



**Daniel J. Dummer** received a BS in physics and a PhD in physics from the University of Minnesota. His thesis research included experimental studies of low-temperature nuclear magnetic ordering. From 1990 to 1993 he performed postdoctoral research at the Max-Planck-Institut für Physik in Munich on low-temperature detectors for elementary particles. From 1993 to 1997 he performed research at the National Institute of Standards and Technology in Gaithersburg, Maryland, on the optical properties of materials. He is currently working on advanced high-speed magnetic recording at Seagate Technology in Minneapolis, Minnesota.